

PCCP

Accepted Manuscript



This is an *Accepted Manuscript*, which has been through the Royal Society of Chemistry peer review process and has been accepted for publication.

Accepted Manuscripts are published online shortly after acceptance, before technical editing, formatting and proof reading. Using this free service, authors can make their results available to the community, in citable form, before we publish the edited article. We will replace this *Accepted Manuscript* with the edited and formatted *Advance Article* as soon as it is available.

You can find more information about *Accepted Manuscripts* in the [Information for Authors](#).

Please note that technical editing may introduce minor changes to the text and/or graphics, which may alter content. The journal's standard [Terms & Conditions](#) and the [Ethical guidelines](#) still apply. In no event shall the Royal Society of Chemistry be held responsible for any errors or omissions in this *Accepted Manuscript* or any consequences arising from the use of any information it contains.

**Dynamics of Energy Transfer and Soft-Landing in Collisions of Protonated Dialanine with
Perfluorinated Self-Assembled Monolayer Surfaces**

Subha Pratihari,^a Dhruv G. Bhakta,^a Swapnil C. Kohale,^a
Julia Laskin,^b and William L. Hase^{a,*}

^aDepartment of Chemistry and Biochemistry
Texas Tech University
Lubbock, Texas 79409-1061

^bPacific Northwest National Laboratory
Physical Sciences Division
P.O. Box 999 K8-88
Richland, Washington, 99352

* To whom correspondence should be addressed: bill.hase@ttu.edu

Abstract

Chemical dynamics simulations are reported which provide atomistic details of collisions of protonated dialanine, $\text{ala}_2\text{-H}^+$, with a perfluorinated octanethiolate self-assembled monolayer (F-SAM) surface. The simulations are performed at collision energies E_i of 5.0, 13.5, 22.5, 30.00, and 70 eV, and incident angles 0° (normal) and 45° (grazing). Excellent agreement with experiment (*J. Am. Chem. Soc.* **2000**, *122*, 9703-9714) is found for both the average fraction and distribution of the collision energy transferred to the $\text{ala}_2\text{-H}^+$ internal degrees of freedom. The dominant pathway for this energy transfer is to $\text{ala}_2\text{-H}^+$ vibration, but for $E_i = 5.0$ eV ~20% of the energy transfer is to $\text{ala}_2\text{-H}^+$ rotation. Energy transfer to $\text{ala}_2\text{-H}^+$ rotation decreases with increase in E_i and becomes negligible at high E_i . Three types of collisions are observed in the simulations: i.e. those for which $\text{ala}_2\text{-H}^+$ (1) directly scatters off the F-SAM surface; (2) sticks/physisorbs on/in the surface, but desorbs within the 10 ps numerical integration of the simulations; and (3) remains trapped (i.e. soft-landed) on/in the surface when the simulations are terminated. Penetration of the F-SAM by $\text{ala}_2\text{-H}^+$ is important for the latter two types of events. The trapped trajectories are expected to have relatively long residence times on the surface, since a previous molecular dynamics simulation (*J. Phys. Chem. B* **2014**, *118*, 5577-5588) shows that thermally accommodated $\text{ala}_2\text{-H}^+$ ions have a binding energy with the F-SAM surface of at least ~15 kcal/mol.

I. Introduction

There are a number of chemical and physical processes which may occur when a protonated peptide ion (peptide- H^+) collides with an organic surface.^{1,2} They include surface-induced dissociation (SID),^{3,4} soft-landing (SL),^{5,6} and reactive-landing (RL).^{7,8} In SID the projectile, energized by its collision with the surface, either dissociates upon impact with the surface (shattering)³ or is scattered into the gas phase and then dissociates. SID is an important experimental tool for determining structural properties of ions,⁹ and energetic and mechanistic information concerning their dissociation pathways.^{10,11} For lower collision energies the ion may adsorb on the surface intact, with or without charge retention, a process referred to as SL.¹² In RL the projectile forms chemical bonds with and chemisorbs on the surface.¹³ SL and RL have a number of important applications, including preparation of protein or peptide arrays, development of novel biosensors and substrates for improved cell adhesion, purification of compounds from complex mixtures, and deposition of mass-selected cluster ions.^{14,15}

Chemical dynamics simulations have been used to study the atomistic details of SID and RL, and compare with experiment.¹⁶⁻²⁸ $Cr(CO)_6^+$ and peptide- H^+ collisions with alkythiolate (H-SAM) and diamond surfaces have been simulated,¹⁶⁻²⁵ and quite good agreement with experiment has been obtained. The distributions of energy transfer to the peptide- H^+ ions, found from the simulations, are in near quantitative agreement with experiment and a shattering mechanism for peptide- H^+ fragmentation is observed in the simulations,^{19,22-26} as deduced from experiment.^{1,29} Though the RL system studied by the simulations is substantially different from that studied experimentally, qualitative agreement is found between experiment and simulations.²⁶

In previous chemical dynamics simulations, energy transfer for collisions of protonated diglycine and dialanine (i.e. gly_2-H^+ and ala_2-H^+) with a perfluorinated alkylthiolate SAM surface (i.e. F-SAM) was studied.³⁰ Though the results agree overall with experiment,³¹ the extent of the agreement is not as good as found for collisions of peptide- H^+ ions with the H-SAM and diamond surfaces. For ala_2-H^+ + F-SAM collision energies in the range of 5 - 30 eV, the simulations give a 13 - 16 % energy transfer to ala_2-H^+ vibration/rotation, while the experimental result is 21 %.³¹ The ala_2-H^+ + F-SAM intermolecular potential, used for the simulations, is represented by a sum of 2-body potentials fit to electronic structure calculations for interactions between CF_4 as a model for the F- and C-atoms of the surface and atoms of NH_3 ,

NH_4^+ , CH_4 , H_2O , and H_2CO as model moieties representing groups of atoms for $\text{ala}_2\text{-H}^+$.³² This potential has two shortcomings: i.e. it only represents the $\text{ala}_2\text{-H}^+$ + F-SAM short-range repulsive potential and does not include the system's long-range attractive potential; and an insufficient number of orientations were included for the electronic structure calculations between CF_4 and the model moieties to uniquely represent the 2-body potential terms between $\text{ala}_2\text{-H}^+$ and the F-SAM. These shortcomings in the $\text{ala}_2\text{-H}^+$ + F-SAM intermolecular potential may affect the energy transfer dynamics obtained from the simulations.

In recent work, a substantially more accurate intermolecular potential was developed for peptide- H^+ ions interacting with perfluorinated hydrocarbon surfaces.³³ More uniquely defined 2-body terms were derived for the ion-surface interaction, which also include the long-range attractions. In the work reported here, the $\text{ala}_2\text{-H}^+$ + F-SAM energy transfer dynamics are re-investigated with this new potential. The goal of the work is multi-fold. The probability for vibration/rotation energy transfer to $\text{ala}_2\text{-H}^+$, obtained from the simulations, is compared with the experimental result.³¹ In addition, the probability that $\text{ala}_2\text{-H}^+$ is temporarily trapped on the F-SAM is investigated in the simulations. Finally, the energy transfer dynamics obtained from these current simulations are compared with the previous findings.³⁰

II. Computational Procedure

A. Surface model and potential energy function

In this work an explicit-atom (EA) model was used to represent the F-SAM surface. This EA model, developed by Borodin and coworkers,³⁴ contains 108 free chains of the $\text{CF}_3(\text{CF}_2)_7\text{S}$ radical adsorbed on a single rigid layer of 441 constrained Au atoms, and has a 3 x 3 unit cell. The S atoms are adsorbed in a rhombic pattern, to correspond to the experimental structure,³⁵ and each S atom interacts with the closest three Au atoms via three individual harmonic stretch potentials. The potential energy function of the F-SAM has both bonded and non-bonded interactions, and is written as:

$$V_{F\text{-SAM}} = \sum_{\text{Stretches}} \frac{k_r}{2} (r - r_e)^2 + \sum_{\text{Bends}} \frac{k_\theta}{2} (\theta - \theta_e)^2 + \sum_{\text{Dihedrals}} \frac{V_n}{2} [1 - \cos(n\varphi - \gamma)] + \sum_{\text{Buckingham}} \left[A \exp(-Br) + \frac{C}{r^6} \right] + \sum_{\text{Klein}} \left[\frac{C_{12}}{(z-z_0)^{12}} + \frac{C_3}{(z-z_0)^3} \right] \quad (1)$$

All the parameters for this model are given in reference 34. This EA model gives a 300 K structure for the FSAM surface which is in excellent agreement with experiment.³⁵

A previous MD simulation, for ala₂-H⁺ adsorbed on the F-SAM surface, showed that the ion penetrates the surface between the alkyl chains.³³ To ensure that this is physically correct, the F-SAM chain-chain intermolecular potential was tested. The CF₄/CF₄ intermolecular potential for different orientations was calculated, at the MP2/aug-ccpVTZ level of theory. As shown in the Supporting Information, these potentials are nearly identical to those given by the F-SAM intermolecular potential of Borodin et al.³⁴ The conclusion from this analysis is that the Borodin et al. F-SAM potential is quite accurate and penetration of the F-SAM by ala₂-H⁺, under thermal conditions, is correct.

Boundary effects were considered by representing the EA F-SAM surface using two different models: periodic boundary conditions (PBC)³⁶ and a frozen outermost layer (rigid border).^{30,37} In the PBC model periodic boundary conditions are applied in the two lateral dimensions of the F-SAM surface. For the rigid border model the exterior chains of the EA F-SAM surface are held rigid, to ensure there are no unphysical distortions of the interior chains. The rigid border model was chosen to be larger in size than the PBC model to account for lateral movement of ala₂-H⁺ on the surface, and had 46 rigid exterior alkyl chains, and 75 interior alkyl chains. The energy transfer dynamics for the surface using both the strategies were compared by studying collisions at $\theta_i = 0^\circ$ and $E_i = 5.0$ and 22.5 eV. These simulation results are statistically the same for the PBC and rigid border models, as found in the earlier study,³⁰ and the rigid border model was used for the majority of the calculations.

The general analytic potential energy function used for the ala₂-H⁺/F-SAM system is given by

$$V = V_{surface} + V_{surface,peptide} + V_{peptide} \quad (2)$$

Where $V_{peptide}$ is the ala₂-H⁺ intramolecular potential, $V_{surface}$ is the potential for the F-SAM surface, and $V_{peptide,surface}$ is the ala₂-H⁺/F-SAM surface intermolecular potential. For the simulations reported here, the AMBER valence force field³⁸ was used for the ala₂-H⁺ intramolecular potential. A local energy minimization procedure, using the VENUS^{39,40} computer program, was carried out to find the minimum energy conformer for the ala₂-H⁺ ion,

the same conformer as found in previous simulations.^{21,22,30} It is well established that the model represented by Eq. (1) gives accurate energy transfer results and dynamics for peptide-H⁺ + surface collisions.^{18,19,21-25} Previous work has shown that the AMBER model for the peptide-H⁺ intramolecular potential gives statistically the same energy transfer dynamics as do the quantum mechanical (QM) AM1 and MP2/6-316* potentials in QM+MM direct dynamics.^{19,22,23}

Following previous studies,^{18,19,21-25} for the current investigation the interaction between ala₂-H⁺ and the F-SAM surface is expressed as a sum of two-body terms between the atoms of ala₂-H⁺ and the C and F atoms of the F-SAM surface. In this explicit atom model, the total intermolecular potential is the sum of atom-atom pair interactions and is given by

$$V = \sum_i \sum_j \left\{ A_{ij} e^{-B_{ij} r_{ij}} + \frac{C_{ij}}{r_{ij}^{n_{ij}}} + \frac{D_{ij}}{r_{ij}^{m_{ij}}} \right\} \quad (3)$$

where i and j refer to atoms belonging to ala₂-H⁺ and the F-SAM, and r_{ij} is the inter atomic distance between the atoms. The $\frac{D_{ij}}{r_{ij}^{m_{ij}}}$ term is added to the Buckingham potential to provide additional flexibility in the potential function. The parameters for the two-body potentials were obtained by fits to intermolecular potential energy curves (IPECs) calculated for CF₄, which represents the F and C atoms of a perfluoroalkane chain, interacting with small molecules chosen to represent functional groups and their atoms present in protonated peptide ions; specifically, CH₄, NH₃, NH₄⁺, and HCOOH.³³ Both the short-range repulsive and long-range attractive interactions were accurately fit for these potentials. The former is important for the energy transfer dynamics for the ala₂-H⁺ + F-SAM collisions,^{18,19,21-25} while the latter may lead to trapping (i.e. soft-landing) of the ala₂-H⁺ ion on the F-SAM surface. The attractive interactions have been considered in previous peptide-H⁺/SAM intermolecular potentials,⁴¹ but not in previous simulations of peptide-H⁺/surface collisions.^{18,19,21-25} Well optimized potential parameters³³ are needed to simulate sticking and consequent desorption of peptides and peptide ions from SAM surfaces. A semiempirical electronic structure calculation⁴² has identified the importance of non-bonded long-range interactions for protein adsorption on functionalized SAM surfaces.

B. Chemical dynamics simulations

The simulations were carried out with the chemical dynamics package VENUS.^{39,40} A beam of $\text{Ala}_2\text{-H}^+$ ions were aimed at the center unit cell of the F-SAM surface, with fixed incident angle θ_i with respect to the surface normal and fixed initial translational energy E_i .⁴³ The $\text{Ala}_2\text{-H}^+$ ion for each trajectory was randomly placed in the cross section of this beam and randomly rotated about its center of mass so that it had an initial random orientation with respect to the surface. The diameter of the beam was chosen so that it overlapped a unit cell on the surface. The azimuthal angle χ , between the beam and a fixed plane perpendicular to the surface, was sampled randomly between 0 to 2π to simulate collisions with different domains of growth on the F-SAM.⁴³ The distance between the center of the beam and the top of the surface was set to 25 Å.

Initial conditions for the vibrational modes of the $\text{Ala}_2\text{-H}^+$ ions were chosen via the quasi-classical normal mode method,⁴⁴ which includes zero-point energies. The excess energy, for each normal mode of vibration, was selected from the mode's 300 K harmonic oscillator Boltzmann distribution. The energy of each mode was partitioned between kinetic and potential by assigning a random phase to the mode. A 300 K rotational energy of $RT/2$ was added to each principal axis of rotation of the ion.

Initial conditions for the F-SAM were chosen by assigning velocities, sampled from a Maxwell-Boltzmann distribution at 300 K, to the surface atoms. The surface was then equilibrated for 8 ps by a molecular dynamics simulation,³⁶ for which the atomic velocities are scaled for the initial 6 ps so the surface temperature corresponds to that for 300 K classical Boltzmann distributions. For the last 2 ps the surface was allowed to equilibrate without any rescaling of velocities. The average final temperature of the surface is 300 ± 5 K. The atomic coordinates and velocities obtained from this equilibration are then used to initiate each trajectory. A Runge-Kutta/Adams-Moulton algorithm, a standard option in VENUS, was used to integrate the trajectories. An integration time step of 0.2 fs was used, which conserved energy to seven significant figures. Trajectories were halted when the separation between the $\text{Ala}_2\text{-H}^+$ ion and the surface reached 40 Å, or when the total integration time of the trajectory reached 10 ps.

Four hundred trajectories were computed for each set of initial conditions with fixed E_i and θ_i to achieve statistically significant results. When a trajectory that scattered off the surface was terminated, the $\text{Ala}_2\text{-H}^+$ ion's final translational energy, E_f , was determined and the ion's internal energy change, ΔE_{int} , was determined by subtracting the initial value of the ion's internal

energy from its final value. The energy transferred ΔE_{surf} is then determined from the energy conservation relationship

$$E_i = E_f + \Delta E_{int} + \Delta E_{surf} \quad (4)$$

Standard deviations of the mean⁴⁵ were calculated for the average percentage energy transfers to ΔE_{int} , ΔE_{surf} , and E_f , to provide uncertainties in the average energy transfer efficiencies. Also determined are the distributions for ΔE_{int} , ΔE_{surf} , and E_f .

The trajectories were analyzed to categorize the nature of the $\text{ala}_2\text{-H}^+$ + F-SAM collision dynamics. Trajectories with only one inner turning point (ITP) in the $\text{ala}_2\text{-H}^+$ + F-SAM collision were identified as direct scattering events.⁴⁶ Those with two or more ITPs were classified as sticking/physisorption or trapping. For the former $\text{ala}_2\text{-H}^+$ desorbed from the F-SAM surface during the 10 ps trajectories, while for the latter $\text{ala}_2\text{-H}^+$ remained trapped on/in the surface when the trajectories were halted. For the sticking/physisorption events, the total time $\text{ala}_2\text{-H}^+$ interacted with the surface was determined. It was identified by the time interval between the time the heavy atom of an $\text{ala}_2\text{-H}^+$ functional group first attains a 5 Å perpendicular distance with its closest surface C-atom and the time this distance becomes 7 Å as $\text{ala}_2\text{-H}^+$ leaves the surface. The $\text{ala}_2\text{-H}^+$ functional groups acquiring these defining distances with the F-SAM surface are -NH_3^+ , $\text{-CH}_2\text{-}$, -NH- , and -COOH , and the respective atoms used to determine the perpendicular distances are N, C, N, and O of OH.

III. Simulations Results

The majority of the simulations were performed for $\text{ala}_2\text{-H}^+$ + F-SAM collisions along the surface normal, with an incident angle θ_i of 0° , the collision angle used in the experiments.³¹ Collision energies E_i of 5.0, 13.5, 22.5, 30.0, and 70.0 eV were studied for this angle of incidence, with 13.5 and 22.5 eV studied in the experiments. The scattered $\text{ala}_2\text{-H}^+$ ions were collected and analyzed independent of the scattering angle θ_f and the azimuthal angle χ . Simulations were also performed for θ_i of 45° , with E_i of 5.0 and 22.5 eV, to study how the angle of incidence affects the collision dynamics. The above simulations were performed with a rigid border model for the F-SAM and simulations at E_i of 5.0 and 22.5 eV, with $\theta_i = 0^\circ$, using periodic boundary conditions (PBC) gave statistically the same results.

Properties investigated in the simulations are the: (1) nature of the $\text{ala}_2\text{-H}^+$ + F-SAM collisions, including the importance of trapping on the surface; and (2) probabilities of transfer of the collision energy to the surface and to the peptide ion's internal degrees of freedom. Each of these is discussed in the following.

A. Types of $\text{ala}_2\text{-H}^+$ + F-SAM collisions and trapping on the surface

Three different types of trajectories were observed in the simulations; i.e. direct scattering of $\text{ala}_2\text{-H}^+$ from the surface, temporary sticking/physisorption of $\text{ala}_2\text{-H}^+$ on the surface and then desorption, and trapping of $\text{ala}_2\text{-H}^+$ on the surface when the trajectories are terminated at 10 ps. The temporary sticking/physisorption events include trajectories for which $\text{ala}_2\text{-H}^+$ penetrates into the F-SAM surface and those for which $\text{ala}_2\text{-H}^+$ is physisorbed on the top of the surface and “hops” on the surface before scattering. The time evolution of a representative trajectory for which $\text{ala}_2\text{-H}^+$ scatters after deep penetration into the F-SAM surface is illustrated in Figure 2. For this trajectory, the $\text{ala}_2\text{-H}^+$ ion spends 0.72 ps inside the F-SAM surface.

Of interest is the relationship between the length of time $\text{ala}_2\text{-H}^+$ interacts with the F-SAM surface and the fraction of the collision energy transferred to ion's internal degrees of freedom, i.e. E_{int} . This is illustrated in Figure 3 for $E_i = 22.5$ eV and θ_i of both 0° and 45° . Somewhat surprisingly, the percentage of E_i transferred to E_{int} is insensitive to the time the ion interacts with the surface. The percentages in Figure 3 are similar to that for all of the scattered trajectories which is 20 % and 23 % for θ_i of 0° and 45° , respectively. For the $\theta_i = 0^\circ$ trajectories the percentages that directly scatter, are temporarily stuck/physisorbed on the surface before scattering, and are trapped on the surface at the 10 ps termination of the trajectories are 29%, 30%, and 41%, respectively. These respective percentages are 76%, 18%, and 6% for the $\theta_i = 45^\circ$ trajectories.

Reported in Table 1 are the percentages of the $\text{ala}_2\text{-H}^+$ ions that remain trapped on the F-SAM surface at the 10 ps termination of the trajectory integration. The trapping probability is strongly dependent on both E_i and θ_i . For normal incidence the trapping probabilities are higher than for the more grazing angle of incidence of 45° . The trapping probability strongly decreases as E_i is increased; e.g. for θ_i of 0° the trapping probability is 84, 41, and 6 % for E_i of 5, 22.5, and 70 eV, respectively. For $\theta_i = 45^\circ$ the trapping probability is 69% at $E_i = 5$ eV, but decreases to 6% at $E_i = 22.5$ eV. Depicted in Figure 4 is the time evolution of a representative trajectory where $\text{ala}_2\text{-H}^+$ remains trapped on the surface when the trajectory is terminated at 10 ps.

Trapping of the $\text{ala}_2\text{-H}^+$ ion occurs when all of E_i is transferred to the ion's internal degrees of freedom and/or to the surface's vibrational modes, so that the ion can not escape from the surface. Transfer of all of E_i is most efficient when the collision energy is low, so that trapping is most probable at the lowest E_i investigated of 5 eV and then decreases as E_i is increased. Transfer of E_i to the surface is more efficient for θ_i of 0° , as compared to 45° , so trapping is more probable for the normal-incidence collision. After the trapped ion becomes equilibrated with the surface, its desorption probability is given by its thermal desorption kinetics. Previous molecular dynamics simulations of $\text{ala}_2\text{-H}^+$ interacting with the F-SAM surface³³ show that the thermally equilibrated $\text{ala}_2\text{-H}^+$ ion has a binding energy as large as ~ 15 kcal/mol.

B. Collision energy transfer probabilities

The average percentages for energy transfer to the projectile's internal degrees of freedom, $P(\Delta E_{int})$, to the surface vibrations, $P(\Delta E_{surf})$, and for energy remaining in the peptide translation, $P(E_f)$, are given in Table 1. Representative probability distributions for $P(\Delta E_{int})$, $P(\Delta E_{surf})$, and $P(E_f)$ are given in Figure 1 for E_i of 13.5, 30, and 70 eV and $\theta_i = 0^\circ$. For θ_i of both 0° and 45° , the percentage energy transfer to the $\text{ala}_2\text{-H}^+$ internal degrees of freedom is independent of the collision energy E_i . For $\theta_i = 0^\circ$ the percentage varies between 17 to 20% and, given the statistical uncertainties, is the same for each E_i . In contrast to this independence of the percentage energy transfer to E_{int} with respect to E_i , for $\theta_i = 0^\circ$ energy transfer to the surface increases and that remaining in $\text{ala}_2\text{-H}^+$ translation E_f decreases as E_i is increased. On the other hand, for $\theta_i = 45^\circ$ energy transfer to the surface and that remaining in E_f are independent of E_i . In considering these results, energy transfer to the surface is expected to be enhanced at the lower collision energies because of sticking/physisorption of $\text{ala}_2\text{-H}^+$ on the F-SAM surface before scattering, which should enhance accommodation of the collision energy with the surface.

As shown in Table 1, the probability of energy transfer to the peptide ion's internal degrees of freedom is nearly the same for the θ_i of 0 and 45 degree simulations. In contrast, for the 45° angle energy transfer to the surface is less probable than at 0° , with more energy remaining in projectile translation. This is the expected result, since normal incidence collisions are expected to transfer more energy to the surface. The probability distributions $P(\Delta E_{int})$, $P(\Delta E_{surf})$, and $P(E_f)$ are compared in Figure 6 for the $\theta_i = 0^\circ$ and 45° simulations at $E_i = 22.5$ eV. It is not clearly understood why the $\theta_i = 0^\circ$ and 45° simulations, at the same E_i give nearly the

same energy transfer probabilities to E_{int} . A conjecture is that it is a result of the “roughness” of the F-SAM surface. Simulations with a perfect diamond {111} surface give strikingly different energy transfer probabilities to E_{int} for $\theta_i = 0^\circ$ and 45° .²⁴ The suggestion has been made that a somewhat “roughened” diamond {111} surface gives similar energy transfer efficiencies to E_{int} for these two angles.²⁴ It is also possible that because the SAMs are relatively soft the collision angle is less important.

The trajectories were analyzed to determine the partitioning of ΔE_{int} to ala_2-H^+ vibration and rotation. For $\theta_i = 0^\circ$, 19% of ΔE_{int} was partitioned to ala_2-H^+ rotation at $E_i = 5$ eV and this percentage was less than 10% for the other E_i , decreasing from 9% at 13.5 eV to 4% at 70 eV. For the $\theta_i = 45^\circ$ collisions the percentage of ΔE_{int} transferred to ala_2-H^+ rotation is 21% for 5 eV and 14% for 22.5 eV, where for the latter the percentage is 8% for the $\theta_i = 0^\circ$ collisions. There is a slight tendency for enhanced transfer to ala_2-H^+ rotation when the incident angle is change to 45° from normal-incidence. In previous simulations of collisions of the $Cr(CO)_6^+$ ion with a n-hexyl thiolate (H-SAM) surface at $\theta_i = 0^\circ$, 27% and 13% of ΔE_{int} was transferred to $Cr(CO)_6^+$ rotation at E_i of 10 and 30 eV, respectively, similar percentages to what are found here. Both the current and former studies show that the percentage of ΔE_{int} transferred to projectile rotation decreases with increase in E_i .

C. F-SAM simulation models

In previous gas/surface scattering simulation studies a rigid border model,^{30,37} periodic boundary conditions (PBC),³⁶ and a finite object⁴⁷ have been used to represent the surface. For the above simulations a rigid border model was used, described above in Section II.A. This model was used to assure that penetration of the F-SAM by ala_2-H^+ , observed in the simulations, did not arise from unphysical flexibility of the F-SAM and to ensure the interior chains do not become unphysically disordered by the colliding ala_2-H^+ projectile. To compare with these simulations, PBC simulations were performed for E_i of 5 and 22.5 eV and $\theta_i = 0^\circ$, the incident angle for which penetration of the F-SAM is most probable. The results are summarized in Table 2, where they are compared with the rigid border simulations. The two models give statistically the same energy transfer and trapping dynamics.

IV. Comparisons with Previous Studies

A. Experiments

In mass spectrometry experiments, Laskin and Futrell³¹ have studied collisions of $\text{ala}_2\text{-H}^+$ with a F-SAM surface at E_i of 4.5, 9.0, 13.5, and 22.5 eV and normal incidence, $\theta_i = 0^\circ$. From an analysis of the experiments they found that the average percentage internal energy transfer to E_{int} of the peptide ion is independent of the collision energy and equal to 21%. For the current simulations at this incident angle the energy transfer to E_{int} is also statistically independent of the 5-70 eV collision energy and equal to 17 to 20%. For the smaller energy range studied by Laskin and Futrell, the simulation percentage is 18 to 20%. The agreement between the experiments and simulations of the percentage energy transfer to E_{int} is quite good.

In the analyses of the experiments, the probability distribution function $P(\Delta E_{int})$ was determined for each of the collision energies. The E_i of 13.5 and 22.5 eV studied in the experiments were also investigated in the simulations, and the experimental and simulation $P(\Delta E_{int})$ for these two E_i are compared in Figure 7. Their agreement is remarkable. The widths of the experimental and simulation distributions are almost identical. For the 13.5 eV collisions, the average energy transfer to E_{int} is 21% in the experiments and 18% in the simulations. If the experimental distribution is shifted to lower energies by 18/21, the two distributions agree quite well. In assessing the agreement and difference between the experimental and simulations, it is important to recognize that for the experiments E_i is not monoenergetic as for the simulations, but has a ± 2 eV width.⁴⁸ This is more important for the lower energy 13.5 eV experiments, for which the disagreement between simulation and experiment is greater.

It is important to point out that the experiments³¹ were performed using a dodecanethiolate F-SAM, while an octanethiolate F-SAM was used for the simulations. However, this difference is not expected to affect the experiment/simulation comparison, since the two F-SAMs are solid-like and have similar ordered structural characteristics. Their melting points, for a transition from an ordered to disordered structure, are higher than the 300 K F-SAM temperature for the experiments and simulations. The H-SAM prepared from octanethiol has a melting point of 327 ± 5 K.⁴⁹ With its stronger intermolecular attractive potential, the melting point for the octanethiol F-SAM should be substantially higher.

It is important to note that the energy transfer dynamics found in these current $\text{ala}_2\text{-H}^+$ + F-SAM simulations are consistent with a range of additional experimental studies of organic and biological ion SID.^{3,4,31,50,51}

B. Simulations

The current simulations for the $\text{ala}_2\text{-H}^+$ + F-SAM collisions, are consistent with, but in overall better agreement with experiment, than the previous simulations.³⁰ As discussed above, experimental studies³¹ of $\text{ala}_2\text{-H}^+$ + F-SAM collisions, for E_i of 4.5 – 22.5 eV and $\theta_i = 0^\circ$, find an average energy transfer to the peptide internal degrees of freedom, ΔE_{int} , of 21%. For these collision conditions, the previous trajectory simulations give a similar, but somewhat smaller, 11-15% transfer to ΔE_{int} . The current simulations are in much better agreement with experiment and give an 18-20% energy transfer percentage to E_{int} for the experimental collision energies. The $\text{ala}_2\text{-H}^+$ + F-SAM intermolecular potential used for the current simulations has more accurate short-range repulsive interactions and also includes long-range attractions,³³ which were not present in the earlier simulation.³⁰ Both the previous and current simulations give distributions of the energy transfer to peptide internal energy, $P(\Delta E_{int})$, whose widths are in very good agreement with experiment.

The principal difference between the current and previous simulations,³⁰ is the importance of short-time sticking/physisorption and long-time trapping of the $\text{ala}_2\text{-H}^+$ ion on the F-SAM surface. Attractive interactions between the peptide ion and the surface were not represented in the $\text{ala}_2\text{-H}^+$ + F-SAM intermolecular potential for the previous study and the current study, with these interactions included, shows that that they may have important effects on the peptide- H^+ + surface collision dynamics, particularly at low collision energies. Temporary or longer time sticking/physisorption//trapping of $\text{ala}_2\text{-H}^+$ on the F-SAM surface did not occur in the previous simulations, since the potential used for these simulations did not include long-range attractive interactions.³⁰ At high collision energies, for which sticking/physisorption//trapping on the F-SAM surface is unimportant, the previous and current simulations give similar results. This is illustrated by the simulations at $E_i = 70$ eV, with $\theta_i = 0^\circ$, for which the current simulation gives percentages energy transfer to E_{int} , E_{surf} , and E_f of 17, 81, and 2%, while the previous simulation study gave 13, 83, and 4%.³⁰ The principal difference between the former and current study is the inclusion of accurate peptide- H^+ + F-SAM attractive interactions in the latter.

V. Conclusions

In concluding, the results of the current simulation study are compared with experiment, the peptide- H^+ + surface dynamics found from the simulations are considered, and questions to be addressed in future studies are suggested. The simulations are performed using a recently developed analytic intermolecular potential for peptide- H^+ + perfluorinated hydrocarbon interactions, fit to ab initio calculations.³³ The potential has more accurate short-range interactions than that developed previously³⁰ and also has long-range attractive interactions which were not included in the previous potential. The former are important to describe energy transfer for the impulsive peptide ion + surface collision, while the latter may lead to sticking, physisorption, or trapping of the ion on the surface.

The simulation results are in overall excellent agreement with the experiments of Laskin and Futrell.³¹ For collision energies E_i in the range of 4.5 to 22.5 eV, they found the percentage of E_i transferred to the $\text{ala}_2\text{-H}^+$ internal energy E_{int} is constant and 21%. For E_i in the range considered in the experiments, the simulations give 18-20%. The previous simulation³⁰ gave 15% for this percentage. Distributions of the probability of energy transfer to E_{int} , $P(\Delta E_{int})$, determined from the experiments and simulations are compared for E_{int} of 13.5 and 22.5 eV and they are in remarkably excellent agreement.

In the simulations trapping of $\text{ala}_2\text{-H}^+$ on the F-SAM surface is observed, which is most important for low energy and normal incident collisions; e.g. for $E_i = 5$ eV and $\theta_i = 0^\circ$ 84 % of the $\text{ala}_2\text{-H}^+$ ions remained trapped on the surface when the trajectories are terminated at 10 ps. Though trapping is not explicitly seen in scattering experiments it is implied by the “loss” of ions which collide with the surface and are not detected.⁴⁸ Analyses of experiments suggest that at low collision energies two-thirds or more of the ions may be trapped on the surface, i.e. see Figure 9 of reference 48. If the trapped ions are thermally accommodated with the surface and have statistical desorption kinetics, their average lifetime on/in the surface is the inverse of their thermal desorption rate constant.⁵² These trapped ions will continuously thermally desorb and provide a weak background to the pulsed signal of the scattered ions observed experimentally. Though these desorption kinetics have not been observed for $\text{ala}_2\text{-H}^+$ trapped on/in the F-SAM surface, there is a record of slow evaporation of larger peptides from SAM surfaces in soft-landing experiments.⁵³

Two unresolved aspects of the $\text{Ala}_2\text{-H}^+ + \text{F-SAM}$ collision dynamics are: the roles of short-time sticking/physisorption and long-time trapping of the ion on the surface; and the dependence of the energy transfer on the incident angle. The long-range attractive interactions between $\text{Ala}_2\text{-H}^+$ and the F-SAM surface lead to short-time scattering events in which the ion penetrates the surface or is physisorbed on the surface without complete accommodation with the surface. Thus, the short-time collision energy transfer dynamics is a composite of the direct scattering events and those with transient sticking/physisorption. The relative importance of these two is expected to depend upon both the ion and the surface. In the previous study³⁰ it was found that, for the directly scattered trajectories, the probability of energy transfer to the surface versus E_i is well represented by the function $P_o \exp(-b/E_i)$, where P_o and b are fitting parameters. However, with sticking/physisorption included in the short-time energy transfer dynamics, this model is incomplete. Some work has been done to develop a more complete model for the energy transfer dynamics at low collision energies.⁵⁴⁻⁵⁶

The dependence of the peptide- $\text{H}^+ + \text{F-SAM}$ energy transfer dynamics on the incident angle, found in the current study, are not well understood. Energy transfer to the peptide- H^+ internal degrees of freedom are not strongly dependent on the incident angle, while energy transfer to the surface and that remaining in peptide- H^+ translation decrease and increase, respectively, with increase in the incident angle from normal at $\theta_i = 0^\circ$ to 45° . The latter two are expected from standard gas-surface energy transfer dynamics.⁵⁷ Understanding these dynamics is further complicated by the greater importance of short-time sticking/physisorption at θ_i of 0° as compared to 45° . More work needs to be done to unravel the dependence of the peptide- $\text{H}^+ + \text{SAM}$ energy transfer dynamics with respect to the incident angle. A conjecture is that the roughness of the SAM surfaces is involved, since for peptide- H^+ scattering off the much smoother diamond $\{111\}$ surface energy transfer to the ion is strongly dependent on the scattering angle.²⁴ In experiments by Herman and co-workers with organic surfaces, it is also observed that energy transfer to ΔE_{int} is nearly independent of the incident angle.^{50,58}

A research topic of much interest in future studies is to understand the role and importance, in SID, of peptide- H^+ ion sticking/physisorption/trapping on the surface. Long-time trapping has been identified as soft-landing (SL),^{5,6} but the current study indicates that short-time sticking/physisorption on the surface influences the SID energy transfer dynamics. An important component of these dynamics, discovered in the current simulations, is penetration of the F-SAM

surface by the $\text{ala}_2\text{-H}^+$ ion. Detailed and careful analyses were performed of the F-SAM model and the F-SAM potential to assure that these results are correct and all aspects of the simulation model were confirmed. A goal for future work is to identify the projectile and surface characteristics which affect the short-time sticking/physisorption and long-time trapping/soft-landing so that their dynamical attributes may be delineated to develop accurate models for the dynamics of peptide- H^+ + surface collisions. It is important to note that an initial simulation has addressed this question.⁵⁹ A particularly difficult, but important, problem for the simulations is to determine the thermal Arrhenius A-factor and activation energy for a trapped ion which is thermally accommodated with the surface. A relatively large desorption activation energy may be expected, since previous molecular dynamics simulations of $\text{ala}_2\text{-H}^+$ interacting with the F-SAM surface show that the thermally equilibrated $\text{ala}_2\text{-H}^+$ ion has a binding energy as large as ~ 15 kcal/mol³³

Acknowledgements

The research at Texas Tech University is based upon work supported by the Robert A. Welch Foundation under grant No. D-0005. Support was also provided by the High Performance Computing Center (HPCC) at Texas Tech, under the direction of Philip W. Smith. The authors also wish to thank the Texas Advanced Computing Center (TACC) for the computational facilities they provided. JL acknowledges support from the U.S. Department of Energy (DOE), Office of Basic Energy Sciences, Chemical Sciences, Geosciences & Biosciences Division.

References

1. R. G. Cooks, T. Ast, T. Pradeep and V. Wysocki, *Acc. Chem. Res.* 1994, **27**, 316-323.
2. J. Cyriac, T. Pradeep, K. Kang and R. Souda, R. G. Cooks, *Chem. Rev.* 2012, **112**, 5356-5411.
3. J. Laskin and J. H. Futrell, *J. Am. Soc. Mass Spectrom.* 2003, **14**, 1340-1347.
4. V. H. Wysocki, K. E. Joyce, C. M. Jones and R. L. Beardsley, *Am. Soc. Mass Spectrom.* 2008, **19**, 190-208.
5. V. Grill, J. Shen, C. Evans and R. G. Cooks, *Rev. Scientif. Instrum.* 2001, **72**, 3149-3179.
6. J. Laskin, P. Wang and O. Hadjar, *Phys. Chem. Chem. Phys.* 2008, **10**, 1079-1090.
7. B. Gologan, J. R. Green, J. Alvarez, J. Laskin and R. G. Cooks, *Phys. Chem. Chem. Phys.* 2005, **7**, 1490-1500
8. P. Wang, O. Hadjar, P. L. Gassman and J. Laskin, *Phys. Chem. Chem. Phys.* 2008, **10**, 1512-1522.
9. V. H. Wysocki, C. M. Jones, A. S. Galhena and A. E. Blackwell, *A. E. J. Am. Soc. Mass Spectrom.* 2008, **19**, 903-913.
10. A. R. Dongre, A. Somogyi and V. H. Wysocki, *J. Mass Spectrom.* 1996, **31**, 339-350.
11. J. Laskin, Energy and Entropy Effects in Gas-Phase Dissociation of Peptides and Proteins. In *Principles of Mass Spectrometry Applied to Biomolecules*; Laskin, J, and Lifshitz, C., Eds.; John Wiley & Sons., Inc.: Hoboken, NJ, 2006.
12. S. A. Miller, H. Luo, S. J. Pachuta and R. G. Cooks, *Science* 1997, **275**, 1447-1450.
13. T. Pradeep, B. Feng, T. Ast, S. J. Patrick, R. G. Cooks and S. J. Pachuta, *J. Am. Soc. Mass Spectrom.* 1995, **6**, 187-194.
14. P. Wang, O. Hadjar and J. Laskin, *J. Am. Chem. Soc.* 2007, **129**, 8682-8683.
15. Q. Hu, P. Wang, P. L. Gassman and J. Laskin, *J. Anal. Chem.* 2009, **81**, 7302-7308.
16. S. B. M. Bosio, and W. L. Hase, *Int. J. Mass Spectrom. Ion Processes* 1998, **174**, 1-9.
17. O. Meroueh and W. L. Hase, *Phys. Chem. Chem. Phys.* 2001, **3**, 2306-2314.

18. O. Meroueh, and W. L. Hase, *J. Am. Chem. Soc.* 2002, **124**, 1524-1531.
19. O. Meroueh, Y. Wang and W. L. Hase, *J. Phys. Chem. A* 2002, **106**, 9983-9992.
20. K. Song, O. Meroueh and W. L. Hase, *J. Chem. Phys.* 2003, **118**, 2893-2902.
21. J. Wang, S. O. Meroueh, Y. Wang and W. L. Hase, *Int. J. Mass Spectrom.* 2003, **230**, 57-64.
22. Y. Wang, K. Song and W. L. Hase, *J. Am. Soc. Mass Spectrom.* 2003, **14**, 1402-1412.
23. K. Park, K. Song and W. L. Hase, *Int. J. Mass Spectrom.* 2007, **265**, 326-336.
24. K. Park, B. Deb, K. Song and W. L. Hase, *J. Am. Soc. Mass Spectrom.* 2009, **20**, 939-948.
25. G. L. Barnes and W. L. Hase, *J. Am. Chem. Soc.* 2009, **131**, 17185-17193.
26. G. L. Barnes, K. Young, L. Yang and W. L. Hase, *J. Chem. Phys.* 2011, **134**, 094106.
27. A. Geragotelis and G. L. Barnes, *J. Phys. Chem. C* 2013, **117**, 13087-13093.
28. W. Ijaz, Z. Gregg and G. L. Barnes, *J. Phys. Chem. Lett.* 2013, **4**, 3935-3939.
29. J. Laskin, T. H. Bailey and J. H. Futrell, *J. Am. Chem. Soc.* 2003, **125**, 1625-1632.
30. L. Yang, O. A. Mazzyar, U. Lourderaj, J. Wang, M. T. Rodgers, E. Martínez-Núñez, S. V. Addepalli and W. L. Hase, *J. Phys. Chem. C* 2008, **112**, 9377-9386.
31. J. Laskin, E. Denisov and J. Futrell, *J. Am. Chem. Soc.* 2000, **122**, 9703-9714.
32. J. Wang and W. L. Hase, *J. Phys. Chem. B* 2005, **109**, 8320-8324.
33. S. Pratihari, S. Kohale, S. A. Vázquez and W. L. Hase, *J. Phys. Chem. B* 2014, **118**, 5577-5588.
34. O. Borodin, G. D. Smith and D. Bedrov, *J. Phys. Chem. B* 2002, **106**, 9912-9922.
35. G.-Y Liu, P. Fenter, C. E. D. Chidsey, D. F. Ogletree, P. Eisenberger and M. Salmeron, *J. Chem. Phys.* 1994, **101**, 4301-4306.

36. Allen, M. P.; Tildesley, D. J. *Computer Simulation of Liquids*; Oxford University Press: New York, 1987.
37. D. Troya and G. Schatz, *J. Chem. Phys.* 2004, **120**, 7696-7707.
38. W. D. Cornell, P. Cieplak, C. I. Bayley, R. Gould, K. M. Merz, D. M. Ferguson, D. C. Spellmeyer, T. Fox, J. W. Caldwell and P. A. Kollman, *J. Am. Chem. Soc.* 1995, **117**, 5179-5197.
39. W. L. Hase, R. J. Duchovic, X. Hu, A. Kormonicki, K. Lim, D.-H. Lu, G. H. Peslherbe, N. K. Swamy, S. R. Vande Linde, A. J. C. Varandos, H. Wang and R. J. Wolfe, VENUS96. A General Chemical Dynamics Computer Program. *QCPE Bull.* **1996**, *16*, 671.
40. X. Hu, W. L. Hase and T. Pirraglia, *J. Comput. Chem.* 1991, **12**, 1014-1024.
41. P. Deb, W. Hu, K. Song and W. L. Hase, *Phys. Chem. Chem. Phys.* 2008, **10**, 4565-4572.
42. D. M. Basalyga and R. A. Latour, Jr. *J. Biomed. Mat. Res.* 2003, **64**, 120-130.
43. S. B. M. Bosio and W. L. Hase, *J. Chem. Phys.* 1997, **107**, 9677-9686.
44. G. H. Peslherbe, H. Wang and W. L. Hase, *Adv. Chem. Phys.* 1999, **105**, 171-201.
45. H. A. Laitinen, *Chemical Analysis*; McGraw-Hill: New York, 1960; p 545.
46. T. Yan and W. L. Hase, *Phys. Chem. Chem. Phys.* 2000, **2**, 901-910.
47. J. T. Paci, H. P. Upadhyaya, , J. Zhang, G. C. Schatz and T. K. Minton, *J. Phys. Chem. A* 2009, **113**, 4677-4685.
48. J. Laskin, E. V. Denisov, A. K. Shukla, S. E. Barlo and J. H. Futrell, *Anal. Chem.* 2002, **74**, 3255-3261.
49. G. Yang and G. Y. Liu, *J. Phys. Chem. B* 2003, **107**, 8746-8759.
50. J. Žabka, Z. Dolejšek and Z. Herman, *J. Phys. Chem. A* 2002, **106**, 10861-10869.
51. J. Laskin and Futrell, J. H. *J. Chem. Phys.* 2003, **119**, 3413-3420.

52. J. I. Steinfeld, J. S. Francisco and W. L. Hase, *Chemical Kinetics and Dynamics*, 2nd Ed.; Prentice Hall: Upper Saddle River, NJ, 1999.
53. J. Alvarez, J. H. Futrell and J. Laskin *J. Phys. Chem. A* 2006, **110**, 1678-1687.
54. J. J. Nogueira, Z. Homayoon, S. A. Vazquez and E. Martinez-Nunez, *J. Phys. Chem. C* 2011, **115**, 23817-23830.
55. M. Monge-Palacios, J. J. Nogueira and E. Martinez-Nunez, *J. Phys. Chem. C* 2012, **116**, 25454-25464.
56. J. J. Nogueira, W. L. Hase and E. Martínez-Núñez, *J. Phys. Chem. C* 2014, **118**, 2609-2621.
57. J. C. Tully, *Surface Science* 1994, **299/300**, 667-677.
58. J. Kubišta, Z. Dolejšek and Z. Hermann, *Eur. Mass Spectrom.* 1998, **4**, 311-319.
59. J. J. Nogueira, Y. Wang, F. Martín, M. Alcamí, D. R. Glowacki, D. V. Shalashilin, E. Paci, A. Fernández-Ramos, W. L. Hase, E. Martínez-Núñez and S. A. Vázquez, *J. Phys. Chem. C* 2014, **118**, 10159–10169.

Table 1. Average Percentage Energy Transfers and Percentage of $\text{Ala}_2\text{-H}^+$ Ions Trapped on the F-SAM Surface^a

E_i (eV)	θ_i	Energy Transfer ^b			Trapping ^c
		$\langle\Delta E_{int}\rangle$	$\langle\Delta E_{surf}\rangle$	$\langle E_f\rangle$	f_{trap}
5	0	19	73	8	84
	45	22	62	16	69
13.5	0	18	71	11	65
22.5	0	20	76	4	41
	45	23	61	16	6
30	0	19	78	3	29
70	0	17	81	2	0

- a. The simulations were performed with the rigid border model for the F-SAM surface. Simulations with PBC at E_i of 5 and 22.5 eV, and $\theta_i = 0^\circ$, give the statistically the same results.
- b. Uncertainties, based on the standard deviation of the mean, vary from 0.1 to 1.1.
- c. The trapping percentage is that for the $\text{Ala}_2\text{-H}^+$ ions which remain trapped on the surface when the trajectories are terminated at 10 ps. The standard deviation in f_{trap} varies from 1.2 to 2.5.

Table 2: Comparison of Rigid Border and PBC Models for the F-SAM Surface

Model	Energy Transfer ^a			Trapping ^b
	$\langle \Delta E_{int} \rangle$	$\langle \Delta E_{surf} \rangle$	$\langle E_f \rangle$	f_{trap}
		$E_i = 5.0 \text{ eV}^c$		
Rigid	19	73	8	84
PBC	21	72	7	86
		$E_i = 22.5 \text{ eV}^d$		
Rigid	20	76	4	41
PBC	17	79	4	40

a. Energy transfer percentages.

b. Percentage of the trajectories that are trapped in/on the F-SAM surface when the trajectories are terminated at 10 ps. The standard deviation in f_{trap} varies from 2 to 3.

c. For $E_i = 5.0 \text{ eV}$, the standard deviation of the mean for the percentages varies from 0.5 to 1.1.

d. For $E_i = 22.5 \text{ eV}$, the standard deviation of the mean for the percentages varies from 0.1 to 0.4.

Figure Captions

Figure 1. Depictions of the optimized structures of the ala₂-H⁺ peptide ion and the F-SAM surface.

Figure 2. Time evolution of a trajectory, at $E_i = 70.0$ eV and $\theta_i = 0.0^\circ$, where ala₂-H⁺ scatters from the F-SAM surface after deep penetration. Snapshots were taken at different times during the trajectory simulation. The color code is: orange–Au; yellow–S; cyan–C; magenta–F; blue–N; red–O; and gray–H.

Figure 3. Scatter plots, for trajectories temporarily stuck/physisorbed on the F-SAM surface, of the percentage of the collision energy transferred to ala₂-H⁺ internal energy E_{int} versus the time ala₂-H⁺ is on/in the surface. Results are reported for $E_i = 22.5$ eV, and $\theta_i = 0.0$ and 45.0° .

Figure 4. Time evolution of a trajectory, at $E_i = 5$ eV and $\theta_i = 0^\circ$, where ala₂-H⁺ remains trapped on/in the F-SAM surface until the 10 ps termination of the trajectory. Snapshots were taken at different times during the trajectory. The color code is the same as in Figure 2.

Figure 5. Probability distributions of the energy transfer to ΔE_{int} , ΔE_{surf} and E_f for $\theta_i = 0^\circ$ and E_i of 13.5, 30.0, and 70.0 eV. Scaling of the y-axis is the same for all nine plots.

Figure 6. Probability distribution functions of ΔE_{int} , ΔE_{surf} and E_f for $E_i = 22.5$ eV and incident angles θ_i of 0 and 45 degrees. Scaling of the y-axis is the same for all six plots.

Figure 7. Comparison of experimental and simulation $P(\Delta E_{int})$ for $E_i = 13.5$ and 22.5 eV for $\theta_i = 0^\circ$. For the curve identified as “0.86 x Expt data” the experimental distribution is scaled by 18/21, where 18 and 21 are the average percentages of E_i transferred to ΔE_{int} in the simulations and experiments, respectively.

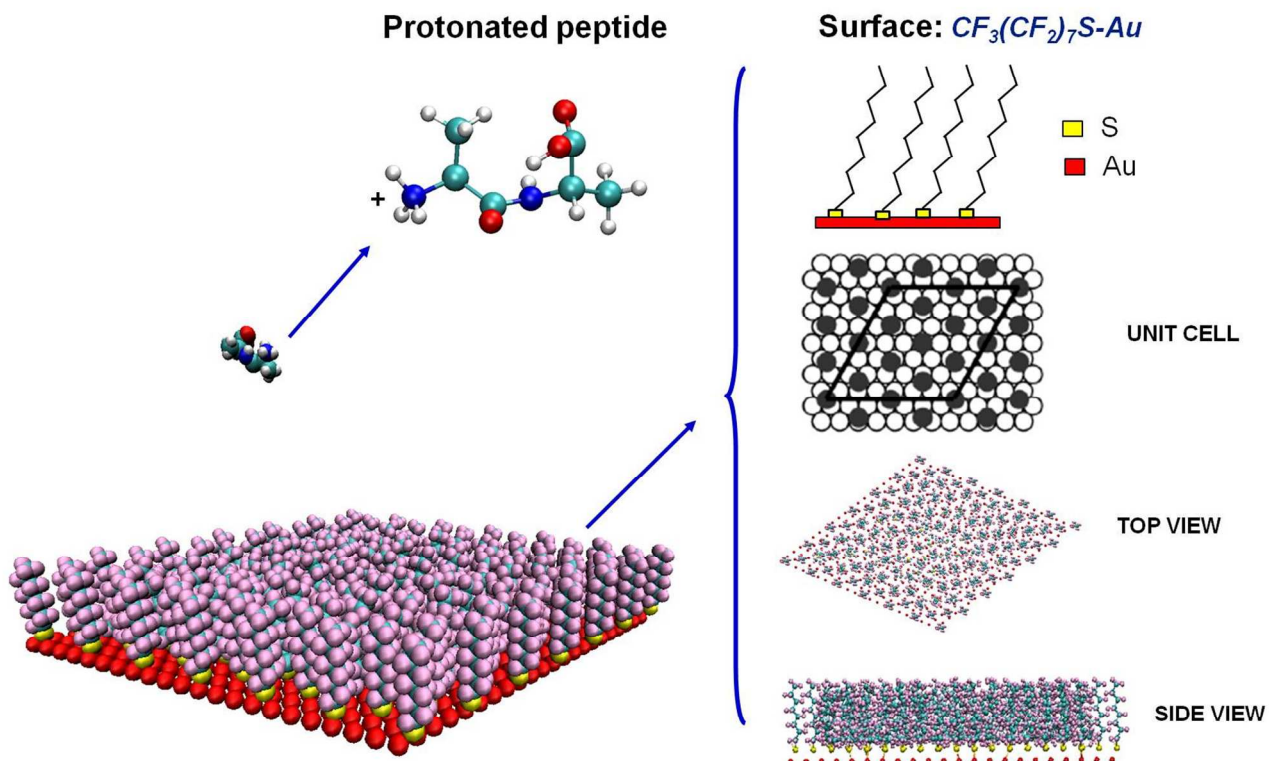


Figure 1

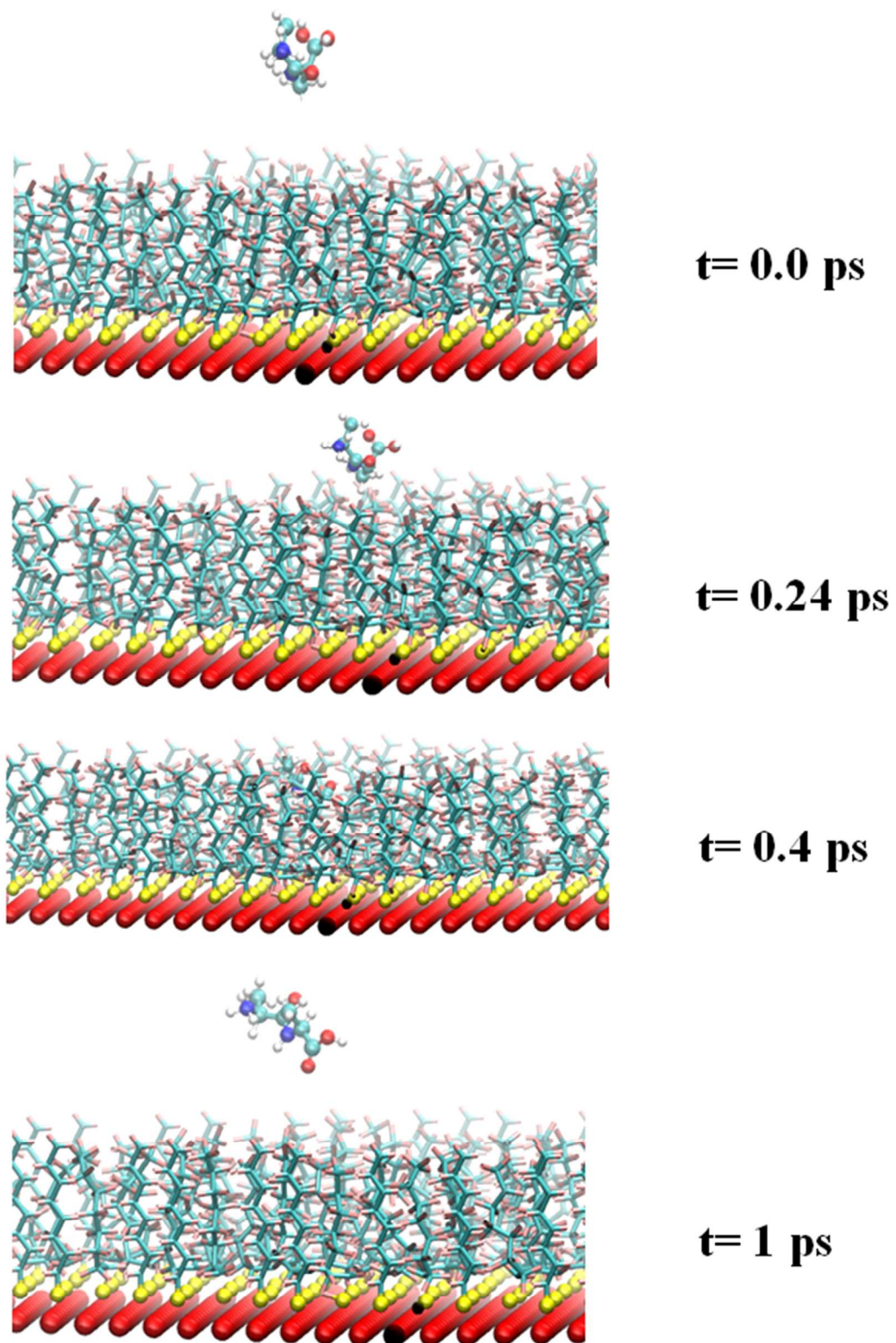


Figure 2

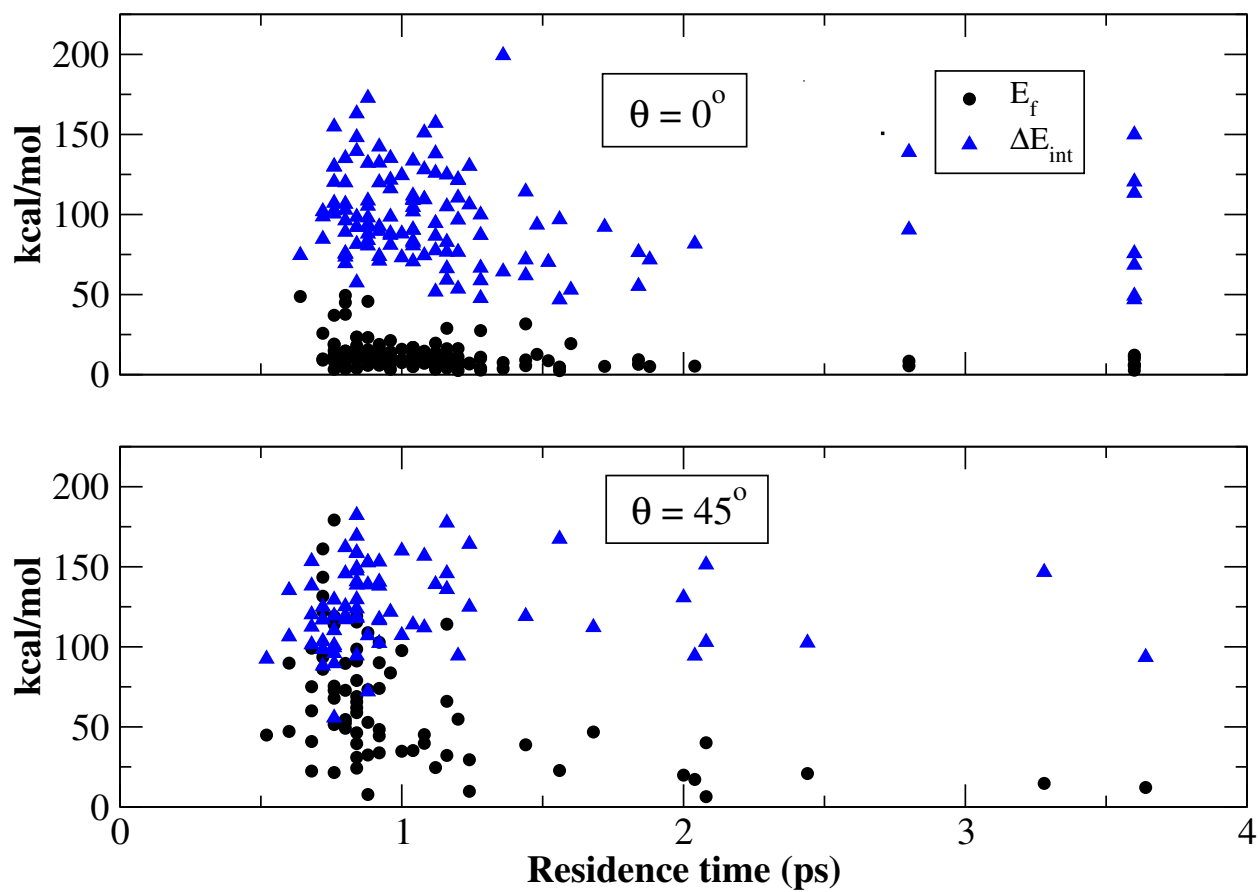


Figure 3

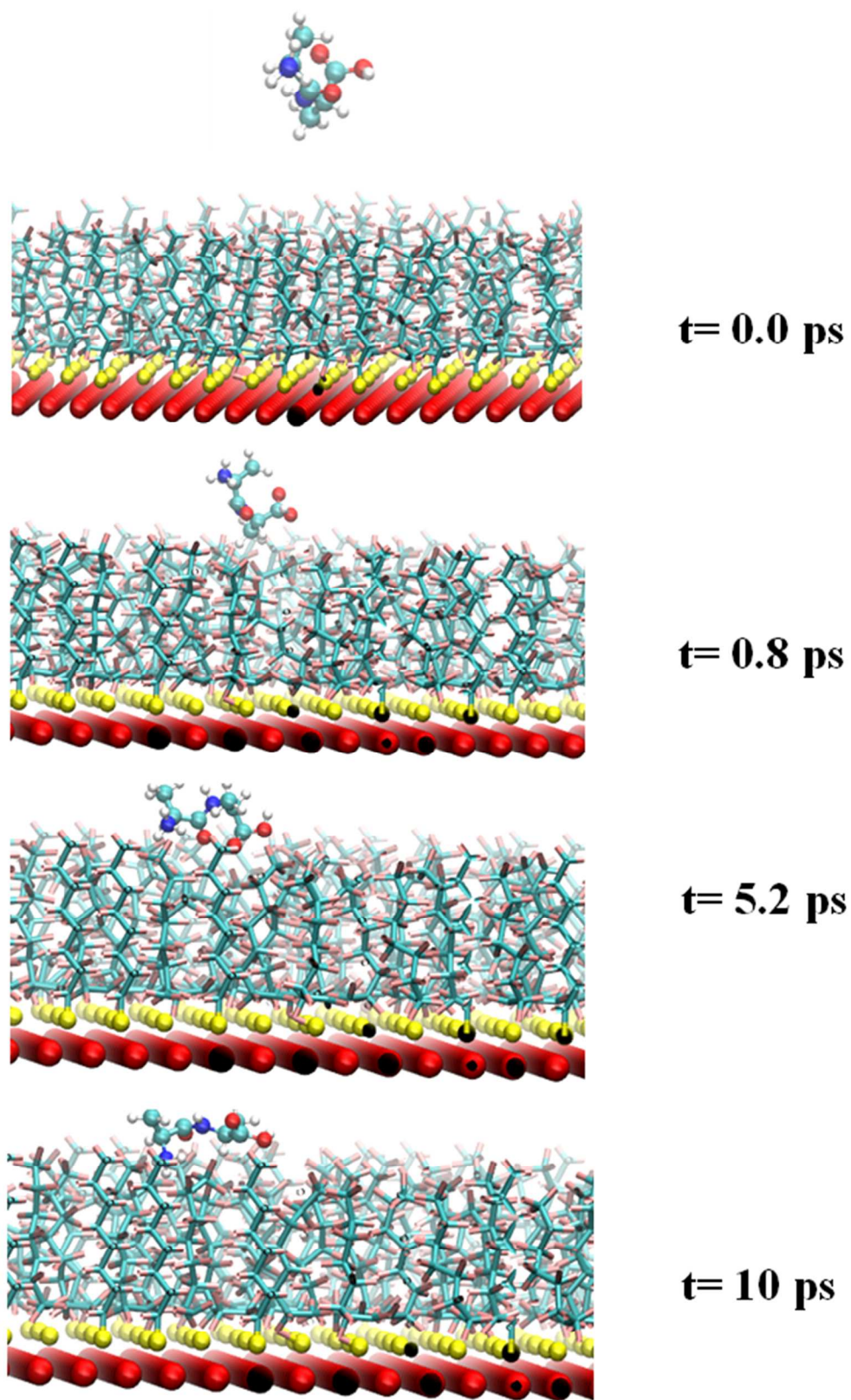


Figure 4

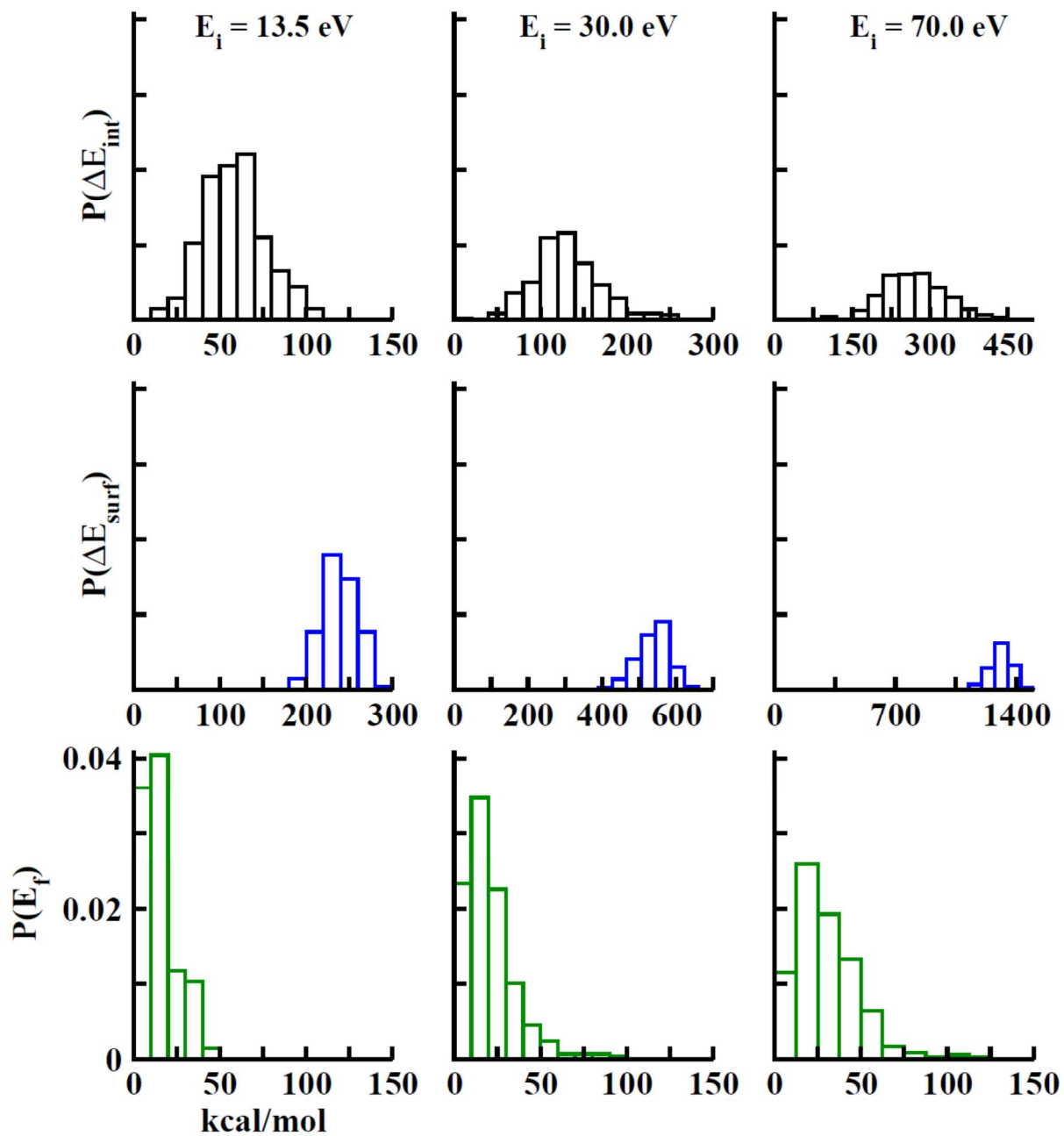


Figure 5

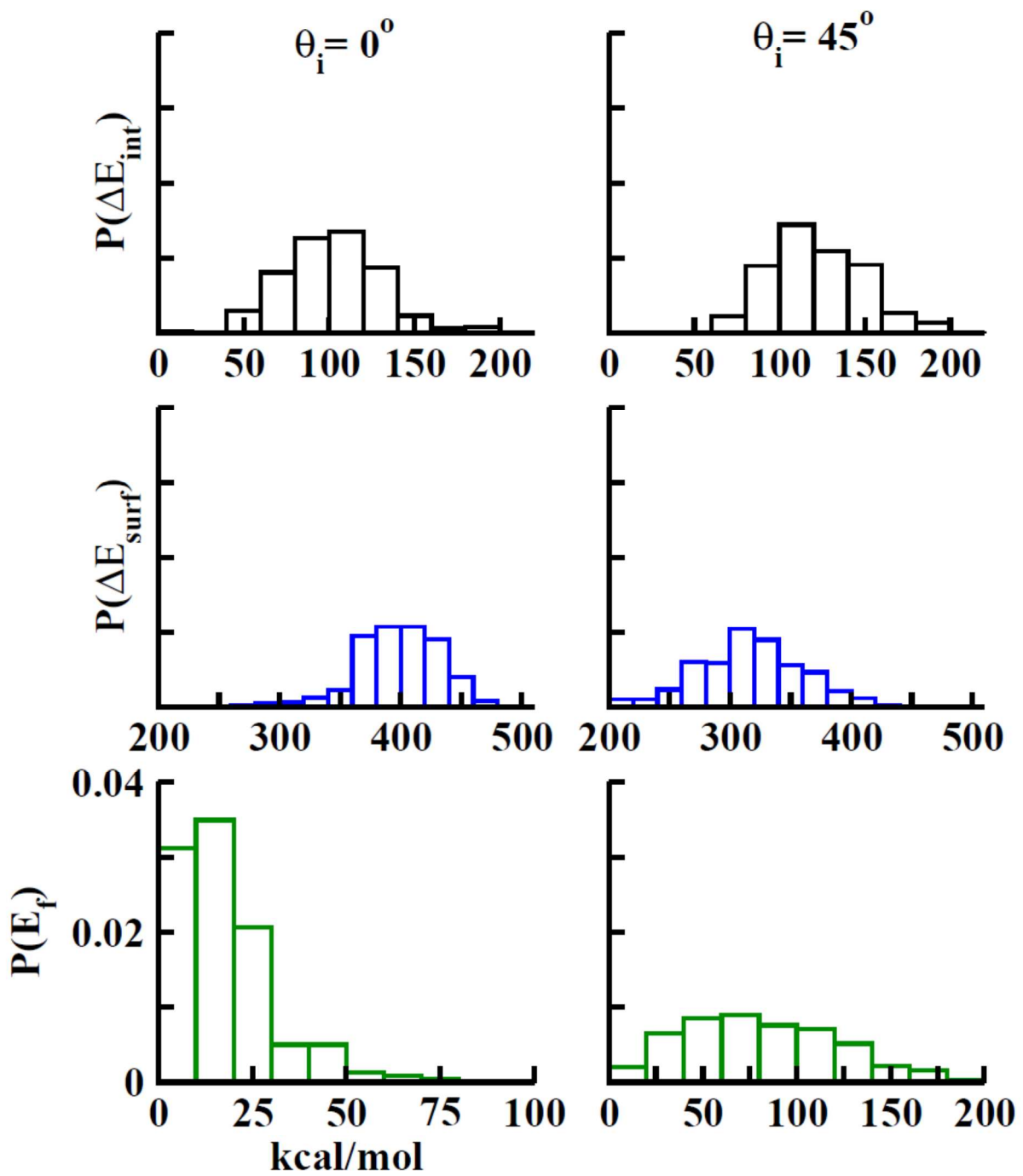


Figure 6

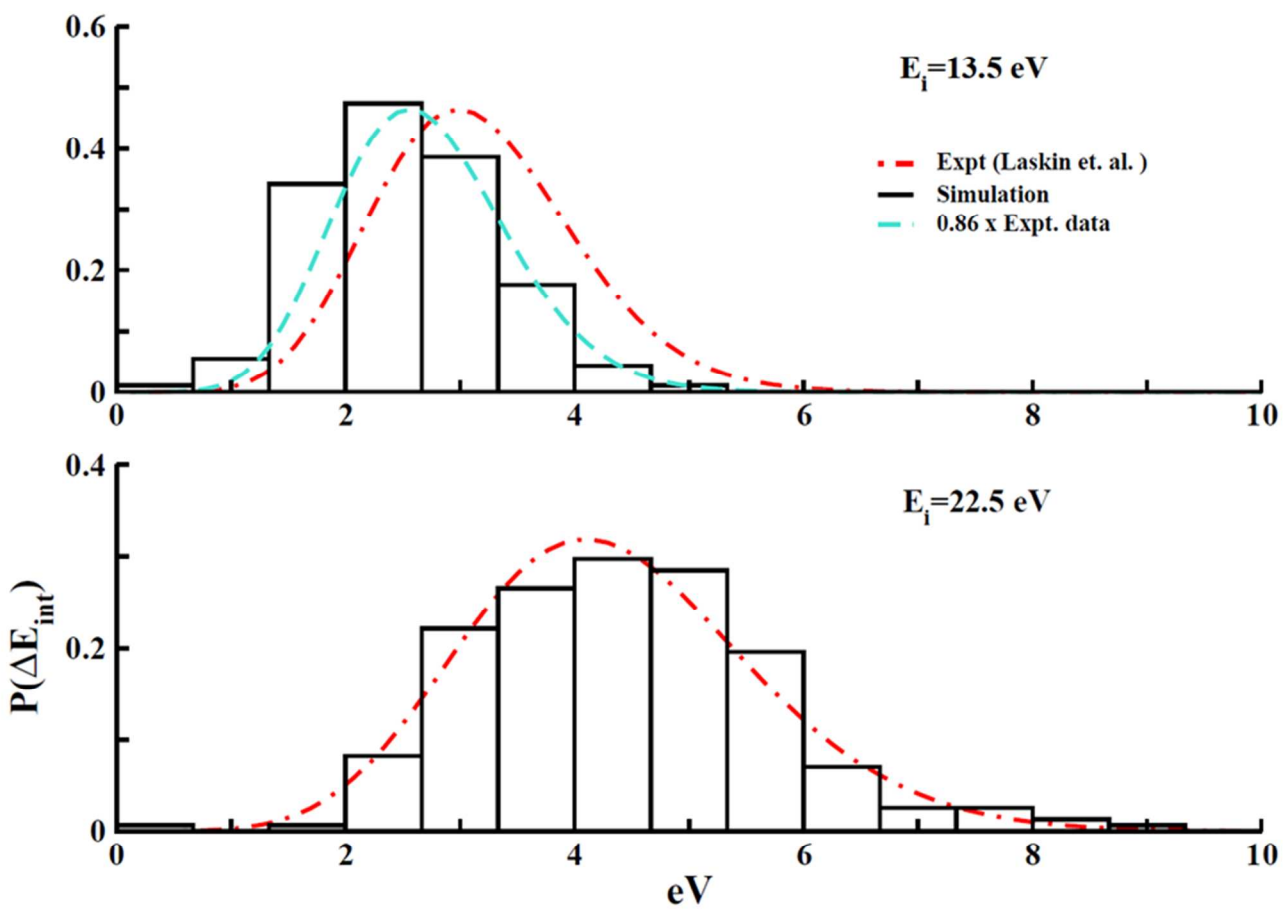
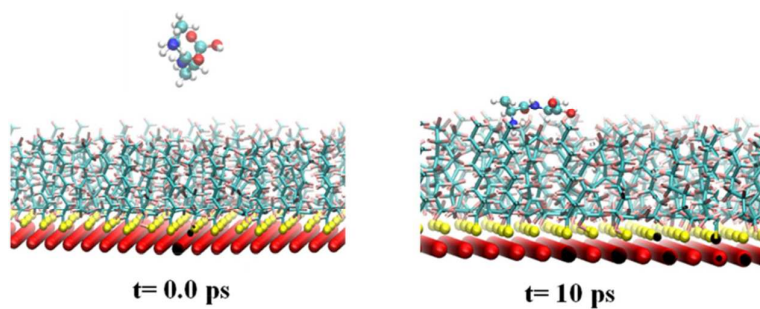


Figure 7



Combined theoretical/experimental study on the collisions of protonated dialanine with a perfluorinated octanethiolate self-assembled monolayer (F-SAM) surface.